



Unleash what's possible.
The guava easyCyte™ 12 flow cytometer is here.

EMD Millipore is a division of Merck KGaA, Darmstadt, Germany



Highly Activated Cytotoxic CD8 T Cells Express Protective IL-10 at the Peak of Coronavirus-Induced Encephalitis

This information is current as of March 29, 2015.

Kathryn Trandem, Jingxian Zhao, Erica Fleming and Stanley Perlman

J Immunol 2011; 186:3642-3652; Prepublished online 11 February 2011;
doi: 10.4049/jimmunol.1003292
<http://www.jimmunol.org/content/186/6/3642>

Supplementary Material <http://www.jimmunol.org/content/suppl/2011/02/11/jimmunol.1003292.DC1.html>

References This article **cites 43 articles**, 19 of which you can access for free at:
<http://www.jimmunol.org/content/186/6/3642.full#ref-list-1>

Subscriptions Information about subscribing to *The Journal of Immunology* is online at:
<http://jimmunol.org/subscriptions>

Permissions Submit copyright permission requests at:
<http://www.aai.org/ji/copyright.html>

Email Alerts Receive free email-alerts when new articles cite this article. Sign up at:
<http://jimmunol.org/cgi/alerts/etoc>

The Journal of Immunology is published twice each month by
The American Association of Immunologists, Inc.,
9650 Rockville Pike, Bethesda, MD 20814-3994.
Copyright © 2011 by The American Association of
Immunologists, Inc. All rights reserved.
Print ISSN: 0022-1767 Online ISSN: 1550-6606.



Highly Activated Cytotoxic CD8 T Cells Express Protective IL-10 at the Peak of Coronavirus-Induced Encephalitis

Kathryn Trandem,* Jingxian Zhao,^{†,‡} Erica Fleming,[†] and Stanley Perlman*^{*,†}

Acute viral encephalitis requires rapid pathogen elimination without significant bystander tissue damage. In this article, we show that IL-10, a potent anti-inflammatory cytokine, is produced transiently at the peak of infection by CD8 T cells in the brains of coronavirus-infected mice. IL-10⁺CD8 and IL-10⁻CD8 T cells interconvert during acute disease, possibly based on recent Ag exposure. Strikingly, IL-10⁺CD8 T cells were more highly activated and cytolytic than IL-10⁻CD8 T cells, expressing greater levels of proinflammatory cytokines and chemokines, as well as cytotoxic proteins. Even though these cells are highly proinflammatory, IL-10 expressed by these cells was functional. Furthermore, IL-10 produced by CD8 T cells diminished disease severity in mice with coronavirus-induced acute encephalitis, suggesting a self-regulatory mechanism that minimizes immunopathological changes. *The Journal of Immunology*, 2011, 186: 3642–3652.

Interleukin-10 is a potent anti-inflammatory cytokine with a crucial role in limiting proinflammatory responses and preventing autoimmune diseases. Although several factors contribute to the anti-inflammatory repertoire, the role of IL-10 is nonredundant. Thus, a spontaneous enterocolitis occurs in mice that are deficient in IL-10, because of florid proinflammatory T cell responses to normal bacterial flora (1). In addition, a deficiency in IL-10 results in exaggerated proinflammatory responses during bacterial, protozoal, and viral infections (2, 3). In most of these studies, IL-10 is produced by CD4 T cells (including effector and regulatory T cells) or by macrophages or dendritic cells, although NK cells have also been identified as an important source in systemic *Toxoplasma gondii* infections (2, 4, 5). Production of IL-10 by IFN- γ ⁺CD4 (Th1) T cells is dependent on strong Ag stimulation; in vitro, these cells required greater dosages of peptide to express maximal levels of IL-10 compared with IFN- γ (6). In addition, IL-10 expression in CD4 T cells is dependent on stimulation via IL-12 and STAT-4 signaling, and requires activation of ERK-dependent pathways.

IL-10 production before complete pathogen clearance contributes to persistent infection. Neutralization of IL-10 in persistent leishmania or lymphocytic choriomeningitis virus infections results in pathogen clearance, with concomitant immunopathological disease in some instances (7–9). Although it is clear that IL-10 has an important role in prolonging pathogen persistence

during chronic infections, only recently has its role in non-persisting virus infections begun to be appreciated. Unlike chronic infections, CD8 T cells, in addition to CD4 T cells, have been identified as major producers of IL-10 in experimental respiratory infections caused by influenza A virus, SV5, and respiratory syncytial virus (10–13); little is known about IL-10 expression by CD8 T cells.

Control of the pathogen and consequent inflammatory response is especially important in infections of the CNS, including viral encephalitis, to minimize tissue damage. Therefore, to investigate the role of IL-10 in acute encephalitis, in particular IL-10 expressed by CD8 T cells, we infected mice with the neurotropic JHM strain of mouse hepatitis virus (14, 15). The J2.2-V-1 variant of this virus produces encephalomyelitis, with progression to a chronic demyelinating disease. Infectious virus is cleared by 10–14 d post-infection (p.i.), although viral Ag and RNA can be detected for months after infection accompanied by low levels of demyelination (14, 16). Inflammation is maximal and extensive throughout the acute phase of the infection (14).

In this article, we demonstrate that expression of IL-10 by CD8 T cells during peak inflammation is not limited to respiratory infections, and that ~50% of IL-10-producing cells in the infected brain are murine hepatitis virus-specific cytotoxic CD8 T cells. In addition, this CD8 T cell-derived IL-10 ameliorates clinical disease in acute encephalitis and subsequent demyelination. IL-10 expression by CD8 T cells requires strong Ag stimulation and signaling through MAPK pathways. Furthermore, using microarray profiling, quantitative RT-PCR (qRT-PCR), and protein analyses, we demonstrate that the fraction of CD8 T cells that produce IL-10 are hyperactivated CD8 T cells. Thus, cytotoxic CD8 T cells may regulate their inflammatory effects during acute infections by producing IL-10, and thereby minimize immunopathological disease.

Materials and Methods

Mice

Specific pathogen-free 6-wk-old Thy1.2 and Thy1.1 C57BL/6 mice were purchased from the National Cancer Institute (Bethesda, MD) and The Jackson Laboratory (Bar Harbor, ME), respectively. Vert-X (C57BL/6 bicistronic IL-10/eGFP) mice were kindly provided by C. Karp (Cincinnati Children's Hospital) (17). IL-10^{-/-} mice (B6.129P2-Il10tm1Cgn/J) were bred at the University of Iowa. Mice were examined and weighed daily. All animal studies were approved by the University of Iowa Animal Care and Use Committee.

*Interdisciplinary Program in Immunology, University of Iowa, Iowa City, IA 52242;

[†]Department of Microbiology, University of Iowa, Iowa City, IA 52242; and

[‡]Institute for Tissue Transplantation and Immunology, Jinan University, Guangzhou 510630, China

Received for publication October 6, 2010. Accepted for publication January 3, 2011.

This work was supported by the National Institutes of Health (Grant NS36592 and Training Grant T32 AI007511-14 to K.T.) and the National Multiple Sclerosis Society.

The sequences presented in this article have been submitted to the Gene Expression Omnibus under accession number GSE25846.

Address correspondence and reprint requests to Dr. Stanley Perlman, Department of Microbiology, BSB 3-730, University of Iowa, Iowa City, IA 52242. E-mail address: stanley-perlman@uiowa.edu

The online version of this article contains supplemental material.

Abbreviations used in this article: CLN, cervical lymph node; MFI, mean fluorescence intensity; p.i., postinfection; qRT-PCR, quantitative RT-PCR.

Copyright © 2011 by The American Association of Immunologists, Inc. 0022-1767/11/\$16.00

Virus and viral titers

Recombinant J2.2-V-1, used in all experiments, was propagated and titered as described previously (18). Mice were inoculated intracerebrally with 500 or 1500 PFU J2.2-V-1 in 30 μ l DMEM.

Preparation of CNS mononuclear cells

Brain mononuclear cells were isolated as described previously (16).

Abs and flow cytometric analyses

All Abs were purchased from BD Pharmingen (San Diego, CA) or eBioscience (San Diego, CA) unless indicated later. NK cells were CD45⁺CD3⁻NK1.1⁺. Macrophages were CD45⁺CD11b⁺Ly6C⁺Ly6G⁻. Neutrophils were CD45⁺CD11b⁺Ly6C⁺Ly6G⁺. MHC class II was detected with anti-I-A/anti-I-E. For detection of intracellular protein expression, CD8 or CD4 T cells were stimulated with 1 μ M peptide S510 or 5 μ M peptide M133, respectively, as previously described (16). IFN- γ , IL-10, TNF, CD107a/b, and granzyme B were detected using Abs purchased from BioLegend (San Diego, CA). For detection of p-ERK, mAb clone D13.14.4E was purchased from Cell Signaling Technology (Beverly, MA). Fc ϵ R1 was detected using anti-DNP IgE (Sigma-Aldrich, St. Louis, MO) followed by rat anti-mouse IgE. M133-specific and S510-specific cells were also detected using PE-conjugated I-A^b/M133 and H-2D^b/S510 tetramers, respectively, obtained from the National Institutes of Health Tetramer Core Facility (Atlanta, GA). Cells were analyzed using a FACSCalibur (BD Biosciences).

Cell separation and sorting

Mononuclear cells were isolated from J2.2-V-1-infected Vert-X/Thy1.2 mice brains at day 7 p.i. Cells from three mice were pooled and CD8

T cells were positively selected or Thy1.2⁺ (CD8 and CD4) T cells were negatively selected using magnetic beads from STEMCELL Technologies (Vancouver, British Columbia, Canada), according to the manufacturer's protocol. GFP⁺, GFP⁻, and CD69⁻ CD8 and/or CD4 T cells were then sorted by a FACSDiva or a FACSria (BD Biosciences). Postsort analysis showed that cells were >99% pure.

In vitro transwell cell culture

Thy1.1 B6 lymph node cells were labeled with 2 μ M CFSE, and 2 \times 10⁶ cells were placed in the lower compartment of anti-CD3 (clone 145-2C11; eBioscience) coated wells. A 0.4- μ m filter separated the two compartments. Thy1.1 B6 splenocytes were pulsed with varying concentrations of S510 peptide (1 μ M to 0 μ M) for 1 h before irradiation with 3000 rad. A total of 2 \times 10⁶ cells was placed in the upper compartment. Thy1.2 CD8⁺ GFP⁺ and CD8⁺GFP⁻ cells were sorted as described earlier, and 2.5 \times 10⁴ cells were placed in the upper compartment with the irradiated splenocytes. A blocking anti-IL-10 mAb (clone JES5-2A5) or an isotype-matched control mAb at 10 μ g/ml (both from BioLegend) was added to some wells. Some cultures were treated with the MEK1/2 inhibitor PD 184161 (ERK1/2) or the p38 inhibitor PD169316 (Cayman Chemical, Ann Arbor, MI). For proliferation studies, lower compartment lymphocytes were stained with anti-CD4-PE and anti-CD8-PerCP, and examined by flow cytometry for CFSE dilution after 48 h. Culture supernatants were harvested for cytokine detection by ELISA.

In vivo GFP conversion

Thy1.2⁺GFP⁺ and Thy1.2⁺GFP⁻ (CD4 and CD8) cells from d7 J2.2-V-1-infected Vert-X mouse brains were sorted as described earlier. Either 1 \times 10⁶ GFP⁺ or 1 \times 10⁶ GFP⁻ cells were transferred in 300 μ l PBS i.v. into

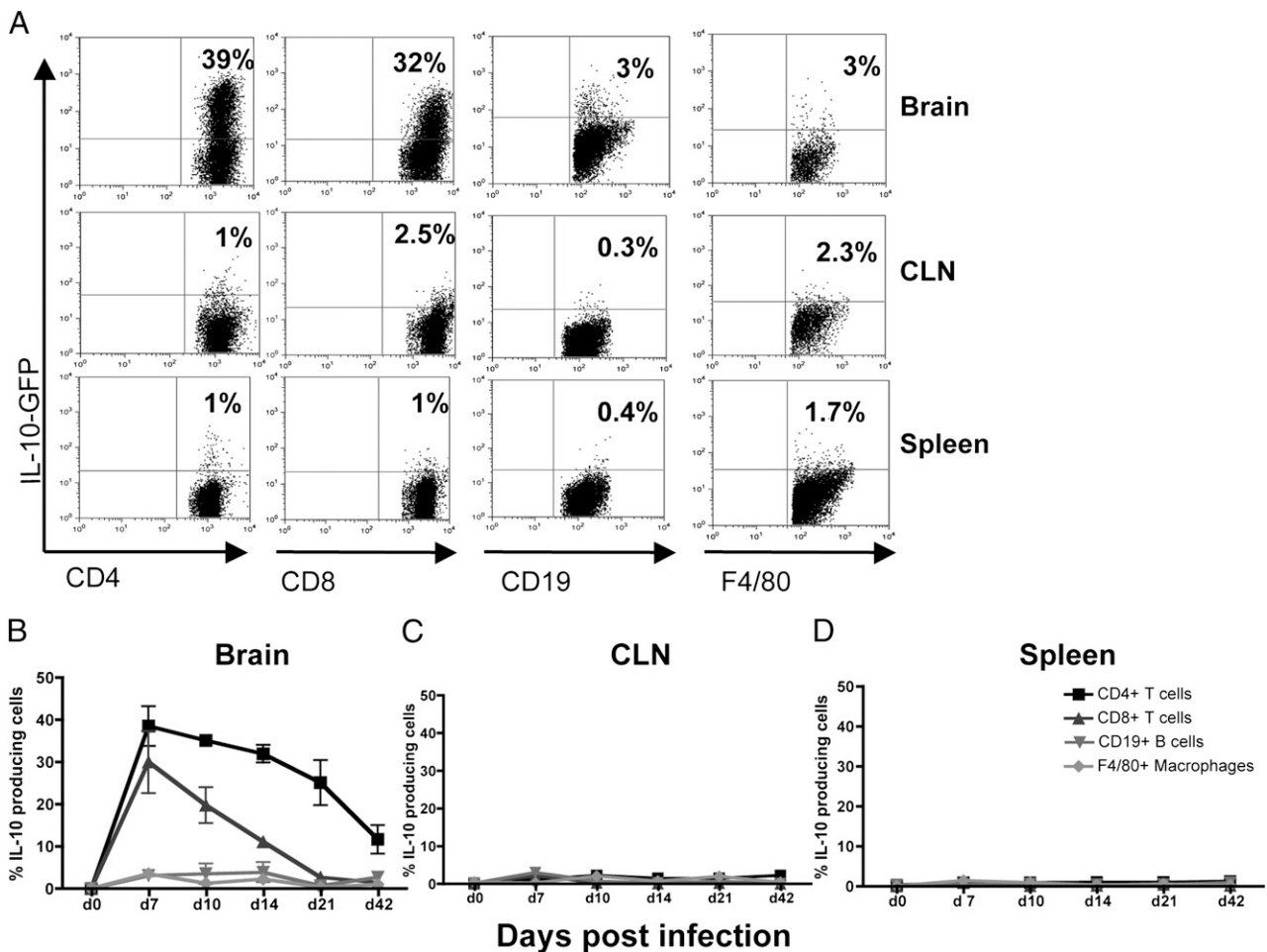


FIGURE 1. IL-10 is produced by cells in the brain and not in the CLN or spleen. Vert-X mice were infected with 500 PFU J2.2-V-1. Brain, CLN, and spleen were harvested at various time points. A, FACS plots of cells stained for various surface markers together with GFP (IL-10) are shown at day 7 p.i. B–D, Frequency of GFP⁺ cells recovered from various cell types at stated time points in the brain (B), CLN (C), and spleen (D). Data are from three separate experiments at each time point with 12 mice/group.

J2.2-V-1-infected Thy1.1⁺ B6 mice at day 1 p.i. Six days later, lymphocytes were harvested, stained, and analyzed by flow cytometry.

ELISA

J2.2-V-1-infected brains were weighed and homogenized directly into 50 mM Tris, 150 mM NaCl, 5 mM EDTA, 1 mM Na₃VO₄, 1% NP-40, and a protease inhibitor mixture (Complete; Roche, Mannheim, Germany). IL-10 and IFN- γ ELISA were performed using reagents and protocols provided by the manufacturer (eBioscience and BioLegend, respectively). Samples were plated in duplicate.

Quantification of demyelination

Blinded quantification of demyelination was performed using Luxol fast blue-stained sections as previously described (19).

Affymetrix microarray

GFP⁺CD8⁺ and GFP⁻CD8⁺ T cells harvested from infected Vert-X mouse brains were sorted at day 7 p.i., as described earlier. RNA was purified using RNeasy columns (Qiagen) according to manufacturer instructions. RNA samples were verified for purity spectroscopically, and the quality of the intact RNA was assessed using an Agilent 2100 Bioanalyzer. RNA for the microarray was processed using a NuGEN WT-Ovation Pico RNA Amplification System together with a NuGEN WT-Ovation Exon Module. Samples were hybridized and loaded onto Affymetrix GeneChip Mouse GENE 1.0 ST arrays. Arrays were scanned with an Affymetrix Model 7G upgraded scanner, and data were collected using GeneChip Operating Software. Complete microarray data have been deposited at the Gene Expression Omnibus under accession number GSE25846 (<http://www.ncbi.nlm.nih.gov/geo/query/acc.cgi?acc=GSE25846>).

Analysis of microarray data

Data from the Affymetrix Mouse Exon 1.0 ST arrays were first quantile normalized and median polished using Robust Multichip Average background correction with log₂ adjusted values. GFP⁺ and GFP⁻ samples were obtained from the same mice, allowing for a paired *t* test. Partek batch correction was used to remove variation caused by the hybridization batch.

Probe sets for exons were then summarized for a specific gene using the median value. After obtaining log₂ expression values for genes, significance testing was performed comparing the two different CD8⁺ T cell groups (IL-10⁺ versus IL-10⁻). False discovery rate correction was applied to all of the *p* values to correct for multiple testing. Significance was assessed by false discovery rate *q* < 0.25 and 2-fold change. Analysis and visualization were done in PartekGS software. Functional assignment of the genes was performed using the "Functional Annotation Tools" in DAVID bioinformatics resources (<http://david.abcc.ncifcrf.gov>) following recommended protocols. Additional analysis was performed using Ingenuity Pathways Analysis (Ingenuity Systems, Redwood City, CA).

qRT-PCR

GFP⁻ and GFP⁺ CD8 T cells were sorted as described earlier, centrifuged, and resuspended in TRIzol Reagent (Invitrogen/Life Technologies, Carlsbad, CA). RNA was extracted and reverse-transcribed using Superscript II (Invitrogen). Relative cytokine transcript quantities were determined by qRT-PCR using SYBR Green (SA Biosciences, Frederick, MD). Primers used for qRT-PCR were as follows: IL-10: forward, 5'-GCGTCGTGATTAGCGATGATG-3'; reverse, 5'-CTCGAGCAAGTCTTTCAGTCC-3'; TNF: forward, 5'-TCAGCCGATTGCTATCTCA-3'; reverse, 5'-CGGACTCCGCAAAGTCTAAG-3'; TLR2: forward, 5'-TTTCGTTTCATCTCTGGAGCA-3'; reverse, 5'-GAGTCCGGAGGGAATAGAGG-3'; TLR3: forward, 5'-ACCTTTGTCTTCTGCACGAACCT-3'; reverse, 5'-AGTTC-TTCACTTCGCAACGCA-3'; TLR4: forward, 5'-TCAGAACTTGAGTGGCTGCA-3'; reverse, 5'-GAGGCCAATTTGTCTCCAC-3'; TLR7: forward, 5'-CAGCCATAACAGCTGACAA-3'; reverse, 5'-TTGCAAA-GAAAGCGATTGTG-3'; CCL2: forward, 5'-AGCACCAGCCAACCTCACT-3'; reverse, 5'-TCATTGGGATCATCTTGCTG-3'; IL-1 α : forward, 5'-CACAACGTGTCGTGAGCGCT-3'; reverse, 5'-TTGGTGTTCCTGGCAACTCCT-3'; IL-1 β : forward, 5'-ACTGTTTCTAATGCCTTCCC-3'; reverse, 5'-ATGGTTTCTTGTGACCCTGA-3'; STAT-4: forward, 5'-CCTACTGGCAGAGAGTCTTTTCC-3'; reverse, 5'-GGTGTGATCAGGAAGGTAGC-3'; perforin: forward, 5'-TTGGCCCATTTGGTGGTAAAG-3'; reverse, 5'-AGTCTCCCCACAGATGTTCTGC-3'; prosaposin: forward, 5'-ACTTCCCACCACCTGATG-3'; reverse, 5'-TAACCTGACAGGCTGTCTCC-3'; HEXA: forward, 5'-GTGCTCATGAAGTCGTAGGTGC-3'; reverse, 5'-CAGGATGTGAAGGAGGTCATTG-3'; hypoxanthine-guanine phosphoribosyltransferase: forward, 5'-GCGTCGTGAT-

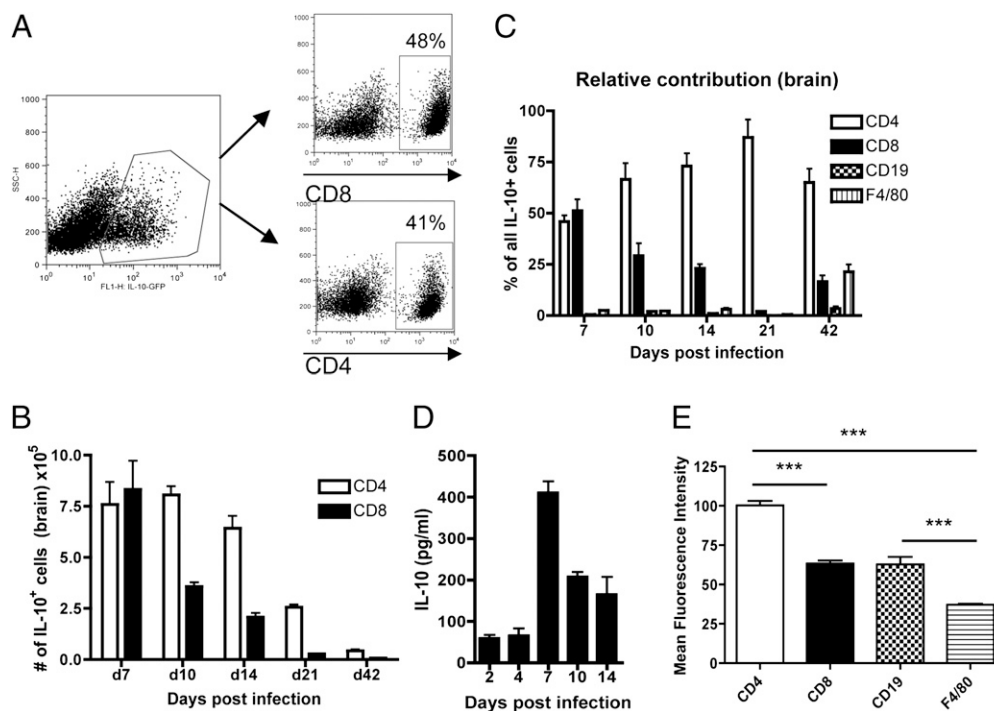


FIGURE 2. IL-10 is produced by T cells in the brain. Vert-X mice were infected with J2.2-V-1 and sacrificed at stated time points. *A*, CNS-derived lymphocytes were examined for IL-10 production at day 7 p.i., as detected by GFP staining. *B*, Total numbers of IL-10⁺ T cells recovered in the brain at different days p.i. *C*, Relative contribution of GFP⁺ cells from various cell types (calculated by multiplying frequency of GFP⁺ by frequency of cell type) in the brain at stated time points. *D*, IL-10 protein levels in brain homogenates were determined by ELISA at the stated time points. *E*, MFI of IL-10 production from various cell types at day 7 p.i. in the brain. ****p* < 0.001. Data are from three separate experiments at each time point with 12 mice/group.

TAGCGATCATC-3'; reverse, 5'-CTCGAGCAAGTCTTTTCAGTCC-3'. Data were analyzed as previously described (18).

Cytotoxicity assay

GFP⁻ and GFP⁺ CD8 T cells were sorted as described earlier. EL4 target cells were peptide pulsed with 1 μ M S510 peptide at 37°C for 1 h and washed. Cytolytic activity was determined using a Cytotox 96 non-radioactive kit (Promega, Madison, WI) according to the manufacturer's instructions. Cytotoxicity assays were performed in triplicate.

Complement depletion

JHMV-immune splenocytes were prepared from B6 or IL-10^{-/-} mice immunized with 3×10^5 PFU wild-type JHMV i.p. 7 d before adoptive transfer. Donor splenocytes were depleted of CD4 T lymphocytes, as previously described (20). Greater than 99% depletion was achieved, as assessed by FACS.

Statistics

Two-tailed unpaired Student *t* tests were used to analyze differences in mean values between groups. Fisher's exact tests were used to analyze differences in survival. One-way ANOVAs were used to analyze differences in multiple groups. All results are expressed as means \pm SEs of the means. Differences of *p* values <0.05 were considered significant.

Results

IL-10 is produced at the site of infection, the brain, by virus-specific T cells

Previous work demonstrated that IL-10 protein is expressed in the CNS of J2.2-V-1-infected mice (5, 21, 22). To identify the cellular sources of IL-10 during the acute and recovery stages of viral encephalitis, we infected IL-10-GFP reporter (Vert-X) mice (5, 13, 17) with J2.2-V-1 and monitored brain, draining cervical lymph nodes (CLN), spleen, and peripheral blood for GFP⁺ cells from days 0–42 p.i. These time points were chosen because virus is cleared by day 14 p.i. and inflammation is mostly resolved by day 42 p.i. (14, 23). We observed the highest frequency of IL-10-producing cells at day 7 p.i., coincident with the onset of the adaptive immune response (Fig. 1A, 1B). Uninfected mice (Fig. 1B) and mice at days 2 and 4 p.i. (data not shown) had very low levels of GFP⁺ cells. At all time points, the highest frequency of GFP⁺ cells was found in the brain, and not in the CLN, spleen, or peripheral blood (Fig. 1B–D, peripheral blood not shown). In addition, T cells accounted for ~90% of IL-10 production (Fig. 2A). Thus, IL-10 is produced by T cells specifically at the site of infection during peak inflammation.

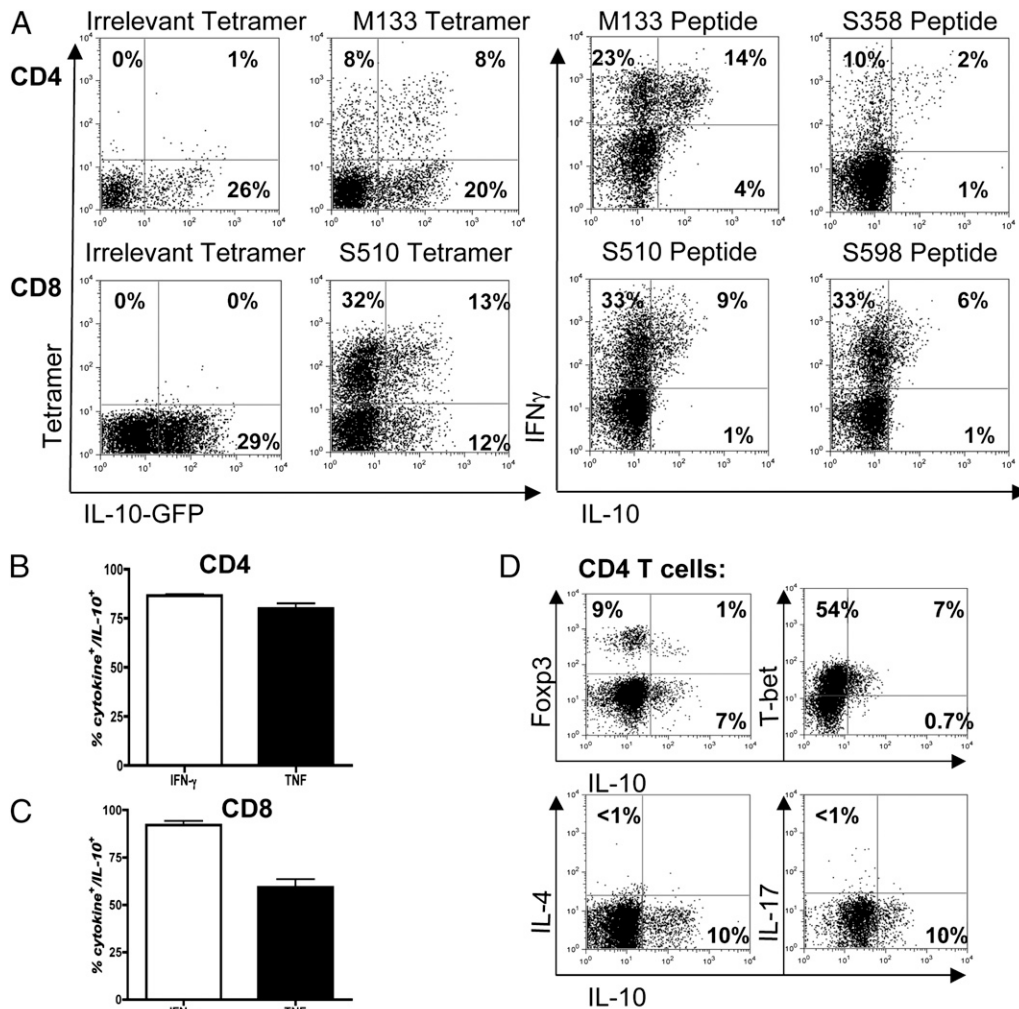


FIGURE 3. IL-10 is produced by virus-specific effector T cells. Vert-X (tetramer staining) or B6 (intracellular cytokine staining [ICS]) mice were infected with 500 PFU J2.2-V-1 and sacrificed at day 7 p.i. For ICS, CNS-derived B6 lymphocytes were prepared and stimulated with the indicated peptides and stained for IL-10, IFN- γ , and TNF expression. *A*, Upper and lower rows are gated on CD4 and CD8 T cells, respectively, and show tetramer/GFP staining (left panels) or cytokine expression after peptide stimulation (right panels). *B*, Frequency of M133-specific CD4 T cells that coproduce IL-10 and IFN- γ or TNF is shown. *C*, Frequency of S510-specific CD8 T cells that coproduce IL-10 and IFN- γ or TNF is shown. *D*, Cells were costained for IL-10, Foxp3, T-bet, IL-4, and/or IL-17, and examined by flow cytometry. FACS plots are gated on CD4 T cells. Data are from four separate experiments with a total of 12 mice analyzed.

During the peak of J2.2-V-1 infection, more CD8 T cells than CD4 T cells infiltrate the CNS (24, 25). Therefore, although a greater fraction of CD4 than CD8 T cells expressed IL-10, ~50% of the IL-10-producing cells were CD8⁺ (Fig. 2B, 2C). The frequency of IL-10⁺CD8 T cells diminished from 40% at day 7 p.i. to <5% at day 21 p.i., whereas the frequency of IL-10⁺CD4 T cells declined more slowly over the course of infection (Fig. 2C). Consistent with the numbers of IL-10-producing T cells, IL-10 protein levels peaked in the brain at day 7 p.i. and diminished thereafter (Fig. 2D). Of note, at all time points, the mean fluorescence intensity (MFI) of GFP expression was greater in CD4 compared with CD8 T cells, demonstrating greater IL-10 production on a per cell basis (Fig. 2E) (17).

Because IL-10 production is generally indicative of a T cell with suppressor function (26), we next determined whether the IL-10⁺CD8 T cells were as potent effectors as IL-10⁻CD8 T cells. Using MHC class I/peptide tetramer staining, we observed that approximately half of the GFP⁺ cells were specific for S510, the immunodominant CD8 T cell epitope recognized in J2.2-V-1-

infected B6 mice (Fig. 3A) (23, 25). In addition, we examined IFN- γ and TNF expression by IL-10⁺CD8 T cells, using intracellular cytokine staining after stimulation with peptides corresponding to S510 and the subdominant epitope, S598. In these assays, we identified IL-10⁺ cells by intracellular cytokine staining because GFP diffused from cells under conditions necessary for IFN- γ and TNF detection. Nearly all of the virus epitope-specific IL-10⁺CD8 T cells expressed IFN- γ and 60–70% also produced TNF (Fig. 3C). Furthermore, cells recognizing the two peptides accounted for almost all of the IL-10 produced by CD8 T cells (Fig. 3A, 3C). Interestingly, IFN- γ and TNF were expressed by virus-specific IL-10⁺CD8 T cells at greater levels per cell than IL-10⁻CD8 T cells (MFI for S510-specific CD8 T cells: IFN- γ ⁺ cells: 418 ± 8 versus 217 ± 4 , $p = 0.0001$; TNF⁺ cells: 305 ± 23 versus 169 ± 11 ; $p = 0.0007$ for IL-10⁺ and IL-10⁻ cells, respectively) consistent with a more highly activated phenotype.

Most IL-10⁺CD4 T cells in the brains of J2.2-V-1-infected mice were effector Th1 T cells, with the majority coproducing IFN- γ and TNF when stimulated by immunodominant (M133) and

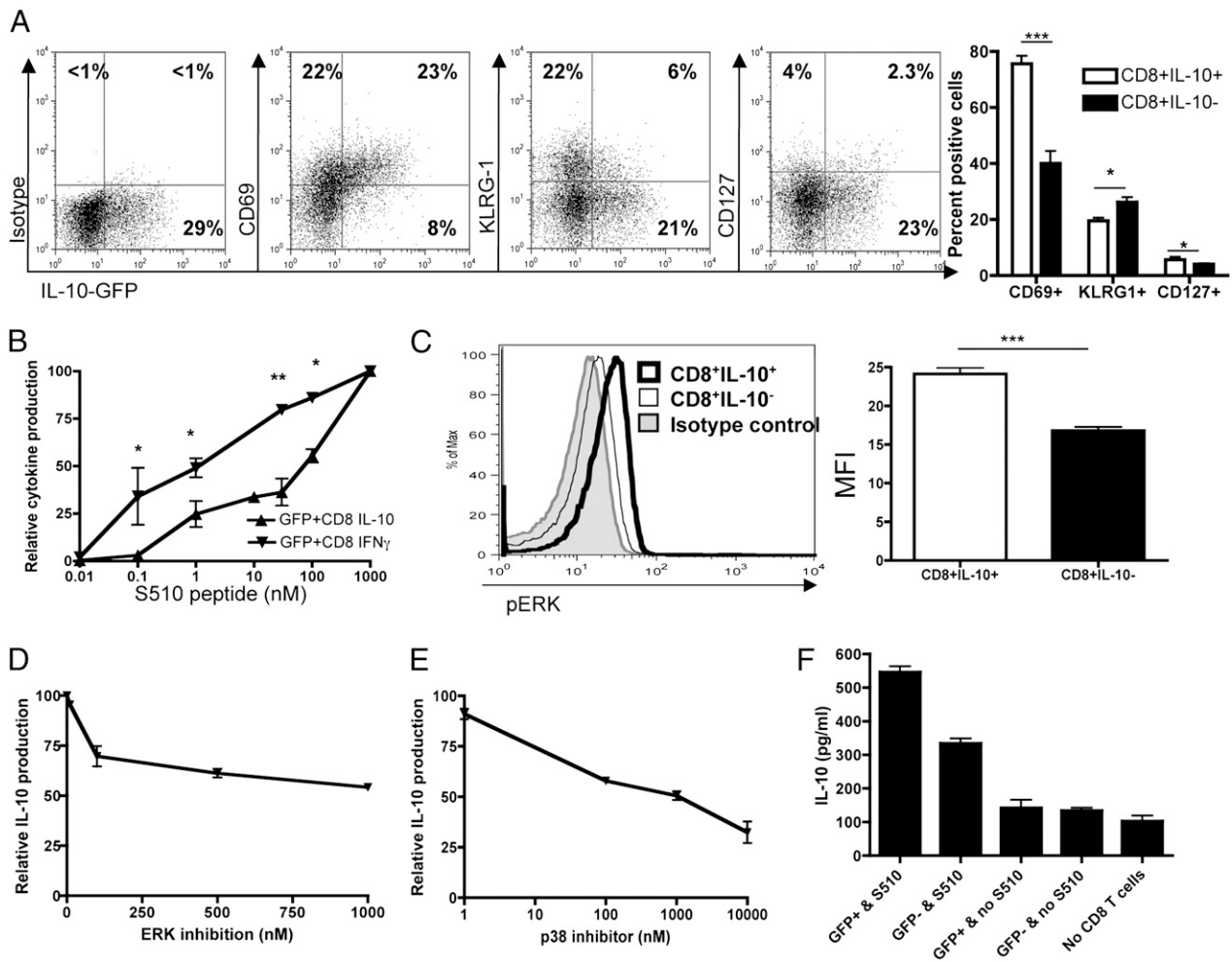


FIGURE 4. CD8 IL-10 production requires recent antigenic stimulation and ERK and p38 MAPK activation for maximal IL-10 production. *A*, Brain lymphocytes from J2.2-V-1 Vert-X mice were harvested at day 7 p.i. and stained for CD69, KLRG-1, and CD127 (IL-7R). Shown are representative FACS plots gated on CD8 T cells. *B*, Brain lymphocytes were obtained from three J2.2-V-1-infected Vert-X mice day 7 p.i. GFP⁺(IL-10⁺) and GFP⁻(IL-10⁻) CD8 T cells were sorted and cultured with varying concentrations of S510 peptide-pulsed irradiated splenocytes for 48 h. IL-10 and IFN- γ production by GFP⁺ CD8 T cells were detected by ELISA. *C*, CNS-derived lymphocytes were examined directly ex vivo for pERK expression. Histogram of pERK in IL-10⁺ CD8 or IL-10⁻CD8 T cells and bar graph displaying MFI for pERK are shown. *D* and *E*, Brain lymphocytes were cultured in vitro as in *B* with stated concentrations of MEK1/2 inhibitor PD184161 (ERK1/2) (*D*) or p38 inhibitor PD169316 (*E*) and analyzed for IL-10 production. *F*, Levels of IL-10 in culture supernatants after 48 h were quantified by ELISA. Samples contained GFP⁺ or GFP⁻ CD8 T cells and irradiated splenocytes in the presence or absence of 1 μ M S510 peptide-pulsed irradiated splenocytes. Control wells included irradiated splenocytes but no added CD8 T cells. * $p < 0.05$, ** $p < 0.01$, *** $p < 0.001$. Data are representative of three to six separate experiments.

subdominant (S358) peptides (Fig. 3A, 3B). Of note, a lower percentage of M133-specific CD4 T cells were identified using tetramer than by intracellular cytokine expression, consistent with low affinity of TCR to MHC class II/peptide binding (27). Approximately 10–15% of IL-10⁺CD4 T cells expressed Foxp3, expressed by regulatory T cells, whereas 85–90% expressed T-bet, consistent with a Th1 phenotype (Fig. 3D). J2.2-V-1 infection induces a strong Th1 cytokine response (21, 28, 29). Only a very low number of cells in the J2.2-V-1-infected brain expressed IL-4 or IL-17; consequently, few, if any, of the IL-10⁺ cells also expressed either of these cytokines (Fig. 3D).

IL-10 production by CD8 T cells requires strong Ag stimulation and signaling through the MAPK pathway

High doses of stimulatory Ag are required for IL-10 compared with IFN- γ production by CD4 T cells (6). CD8 T cells produced IL-10 at the site of infection and production was maximal at the peak of the inflammatory response (Fig. 1). Furthermore, a greater frequency of IL-10⁺CD8 T cells expressed CD69, a marker of recent antigenic stimulation, compared with IL-10⁻CD8 T cells (Fig. 4A). In addition, CD127 expression was slightly higher and KLRG-1 expression modestly lower on IL-10⁺CD8 T cells, suggestive of a memory progenitor phenotype (Fig. 4A) (30). This raised the possibility that IL-10 production in CD8 T cells was also dependent on strong Ag stimulation. To assess this possibility, we examined IL-10 production by stimulating GFP⁺CD8 T cells with irradiated splenocytes pulsed with varying S510 peptide doses directly ex vivo for 48 h. Indeed, ~100-fold more peptide was required to produce 50% maximal levels of IL-10 compared with IFN- γ (Fig. 4B).

Strong signaling through the TCR activates the MAPK pathway, consisting of ERKs (ERK1/2), JUN N-terminal kinases, and p38 (4, 31). Because IL-10 production was dependent on stimulation with high Ag concentrations, we next examined whether the MAPK pathway was activated under conditions of high Ag stimulation. As shown in Fig. 4C, the level of p-ERK was greater in IL-10⁺ CD8 T cells than in IL-10⁻CD8 T cells when cells were stained directly ex vivo for p-ERK1 and p-ERK2 (p44/42).

To demonstrate a functional role for ERK, we stimulated GFP⁺ CD8 T cells with irradiated splenocytes pulsed with S510 peptide in the presence of varying concentrations of the ERK inhibitor PD184161 for 48 h in an in vitro assay. PD184161 is a potent, selective inhibitor of MEK1/2, the upstream kinases of ERK1/2 (32). As seen in Fig. 4D, selective inhibition of ERK phosphorylation decreased IL-10 production by ~50%. Another MAPK, p38, was also involved in IL-10 expression because stimulation of GFP⁺CD8 T cells with S510 peptide in the presence of a selective p38 inhibitor (PD169316) (33, 34) decreased IL-10 production by 75% (Fig. 4E). Decreased amounts of IL-10 did not reflect a loss of cell viability because only low levels of apoptosis (~10%), as assessed by Annexin V and 7-AAD staining, were detected in all cultures (data not shown). Therefore, inhibition of either ERK1/2 and p38 MAPK pathways decreased IL-10 expression by CD8 T cells.

IL-10 production by CD8 T cells is transient

Unexpectedly, when we stimulated GFP⁻CD8 cells for 48 h with high concentrations of peptide S510, we detected IL-10 in the cultures, suggesting that the sorted GFP⁻CD8 T cells had converted to IL-10-producing cells after high antigenic stimulation

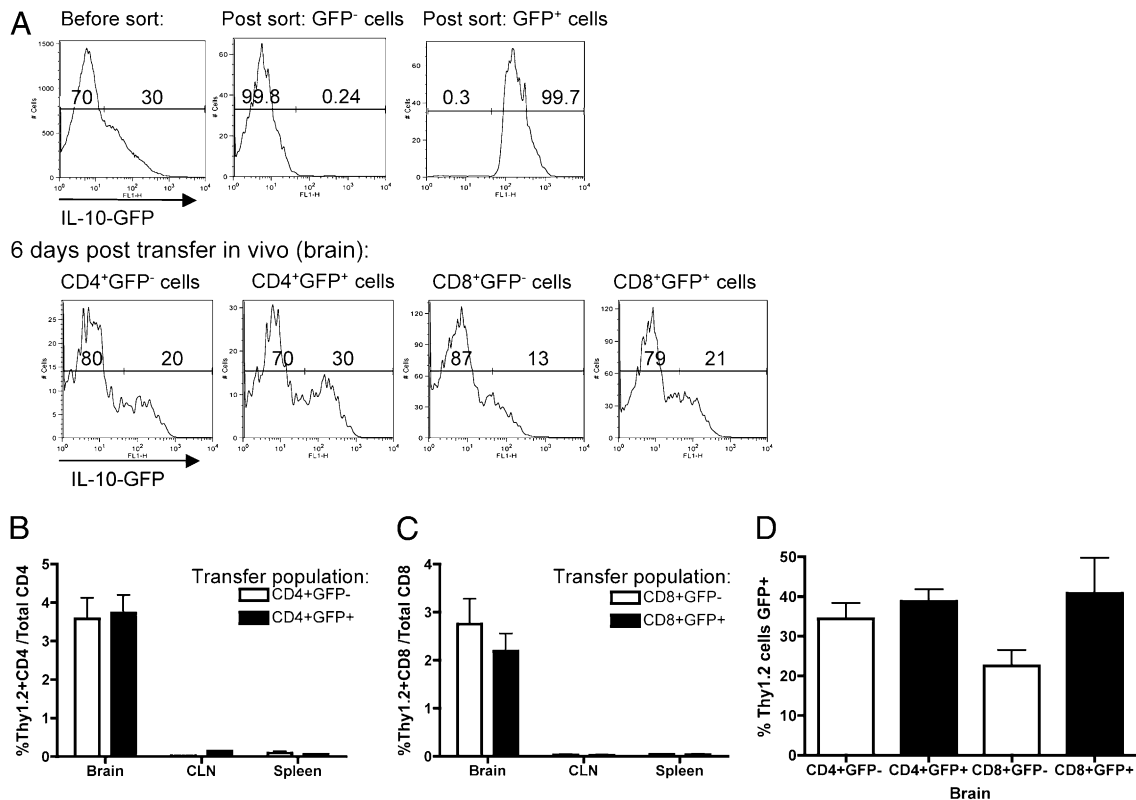


FIGURE 5. The production of IL-10 by effector CD8 and CD4 T cells is transient in vivo. Brain lymphocytes were obtained from three J2.2-V-1-infected Vert-X mice day 7 p.i. GFP⁺(IL-10⁺)Thy1.2 and GFP⁻(IL-10⁻)Thy1.2 CD4 and CD8 T cells were sorted and adoptively transferred (AT) i.v. into a J2.2-V-1-infected Thy1.1 mouse at day 1 p.i. Six days later, mice were sacrificed. *A*, Histograms show GFP expression before and after sorting, and 6 d after AT. *B* and *C*, Frequency of AT CD4 (*B*) or CD8 (*C*) Thy1.2 lymphocytes in the brain, CLN, and spleen. *D*, Frequency of AT Thy1.2⁺ cells that were GFP⁺ in the brain. White bars denote mice originally receiving GFP⁻ Thy1.2 lymphocytes; black bars are mice that originally received GFP⁺ Thy1.2 lymphocytes. Data are representative of five separate experiments with a total of 10 mice analyzed.

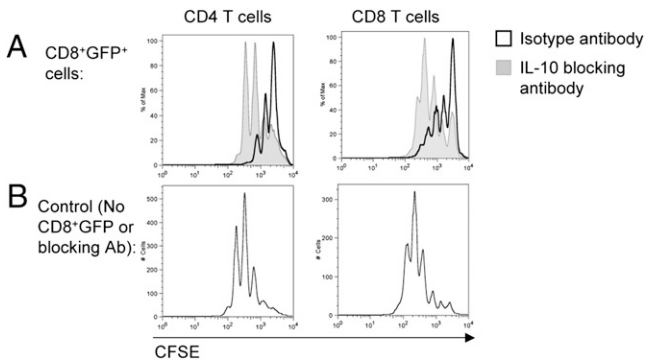


FIGURE 6. IL-10 expressed by cytotoxic CD8 T cells is suppressive directly ex vivo. CNS-derived GFP⁺(IL-10⁺) CD8 T cells were sorted and cultured with S510-peptide pulsed-irradiated splenocytes in an upper transwell compartment, whereas CFSE-labeled naive lymphocytes were placed in the bottom compartment and stimulated with anti-CD3 Ab for 48 h. Cells were cultured with blocking anti-IL-10 Ab or with an isotype control. Histograms show CFSE dilution of lower compartment CD4 and CD8 lymphocytes. The upper compartment contained GFP⁺CD8 (A) or no CD8 T cells (B). Data are representative of three separate experiments.

(Fig. 4F). Consistent with this result, some of the cells that were initially GFP⁻ expressed GFP after in vitro culture (data not shown). IL-10 expression did not occur in the absence of peptide S510 or in cultures without sorted CD8 T cells (Fig. 4F).

To investigate whether this phenotypic plasticity also occurred in the infected animal, we transferred Thy1.2 GFP⁺ T cells or Thy1.2 GFP⁻ T cells into J2.2-V-1-infected Thy1.1 mice. Mice were sacrificed 6 d after transfer, and Thy1.2 CD8 and CD4 T cells were examined for GFP expression. Mice were analyzed at day 7 p.i. to allow sufficient time for proliferation of transferred cells. The highest frequency of transferred cells, whether initially GFP⁺ or GFP⁻, was detected in the infected brain compared with the CLN or spleen (Fig. 5B, 5C). In addition, transferred GFP⁺ and GFP⁻ T cells were detected in the brain at similar frequencies, suggesting that IL-10⁺ cells were not more prone to cell death. Remarkably, IL-10 production was transient in both CD8 and CD4 T cells, so that some cells that were initially IL-10⁺ (GFP⁺) became GFP⁻ and some of the IL-10⁻ (GFP⁻) T cells became GFP⁺ (Fig. 5A, 5D). Of note, T cells that were originally IL-10⁺ or IL-10⁻ appeared to proliferate equally, even though IL-10 inhibited proliferation in vitro. This equivalent proliferative ability may reflect IL-10 plasticity, because similar frequencies of cells were IL-10⁻ after 6 d in mice.

IL-10 produced by CD8 T cells is suppressive

Because J2.2-V-1-specific IL-10⁺CD8 T cells coproduced IFN- γ and TNF, we assessed whether the IL-10 produced by these cells was immunosuppressive or, alternatively, immunostimulatory (35, 36) in an in vitro proliferation assay. Using a transwell assay system, we placed GFP⁺CD8 T cells in the upper compartment with peptide-stimulated irradiated splenocytes. CFSE-labeled naive lymphocytes were incubated in the lower compartment of an anti-CD3-coated plate. As expected, naive CD4 and CD8 T lymphocytes proliferated in the presence of anti-CD3 stimulation as demonstrated by CFSE dilution (Fig. 6). Proliferation was inhibited if GFP⁺CD8 T cells were present in the culture. Inhibition was mediated by IL-10, because the presence of a blocking IL-10 Ab largely reversed the inhibitory effect.

CD8 T cells that produce IL-10 express a transcriptional hyperactivated signature

IL-10⁺CD8 T cells were most abundant during the peak of inflammation (Fig. 1B) and coproduced inflammatory cytokines (Fig. 3C), and IL-10 expression was dependent on MAPK activation and high Ag load (Fig. 4). These results, coupled with data showing that these cells were immunosuppressive (Fig. 6), raised the possibility that the IL-10⁺CD8 T cells were more highly activated than IL-10⁻CD8 T cells. To evaluate this possibility, we compared patterns of global transcription in IL-10⁺ and IL-10⁻ CD8 T cells by microarray analyses.

For this purpose, CNS-derived CD8 T lymphocytes were pooled from three mice and sorted for recent IL-10 production as detected by GFP expression to high purity (>99%) at day 7 after J2.2-V-1 infection. Genome-wide microarray studies were performed on mRNA purified from three pools of lymphocytes. We performed statistics on the gene expression data and found 384 genes statistically significantly increased and 25 genes decreased in IL-10⁺ cells compared with IL-10⁻ cells (Supplemental Table I). Using DAVID and Ingenuity Pathways Analysis to evaluate the gene sets identified, we detected significant changes in several pathways of immune activation and regulation (Table I, Supplemental Table I). Notably, there was increased expression of genes encoding cytokines (*Il1a*, *Il1b*, *Il10*, *Il18*, *Tnf*), chemokines (*Ccl2*, *Ccl3*, *Ccl6*, *Ccl7*, *Ccl8*, *Ccl9*, *Ccl12*, *Cxcl2*, *Cxcl4*, *Cxcl6*, *Cxcl9*), immune sensor molecules (*Tlr1*, *Tlr2*, *Tlr3*, *Tlr4*, *Tlr6*, *Tlr8*, *Tlr13*, *Fcer1g*, *Fcgr1*), and lysosomes/endocytosis (*Abca1* [ATPv], *Gla*, *Hexa/b*, *Lamp1/2* [CD107a/b], *Acp2*, *Prf1*, *Psap*, *Lgmn*, *ctsb/c/h/l/z* [cathepsin B/C/H/L/Z]), suggesting that cells expressing

Table I. Increased gene expression in inflammatory pathways in IL-10⁺CD8 T cells compared with IL-10⁻CD8 T cells

KEGG Pathway	No. of Genes	% of Input	p Value	Genes Upregulated	Genes Downregulated
Lysosome	21	5.9	2.15E-10	<i>CTSZ</i> , <i>LIPA</i> , <i>PSAP</i> , <i>HEXA</i> , <i>GUSB</i> , <i>LGMN</i> , <i>HEXB</i> , <i>ACP2</i> , <i>CD63</i> , <i>ASAHI</i> , <i>GNS</i> , <i>LAMP1</i> , <i>SLC11A1</i> , <i>CTSL</i> , <i>LAMP2</i> , <i>CD68</i> , <i>GLA</i> , <i>ATP6V0A1</i> , <i>CTSC</i> , <i>CTSB</i> , <i>CTSH</i>	
Cytokine–cytokine receptor interaction	26	7.3	4.69E-08	<i>CCL3</i> , <i>CCL2</i> , <i>TNF</i> , <i>IL18</i> , <i>CCR1</i> , <i>CXCL2</i> , <i>CCL9</i> , <i>CXCL9</i> , <i>CCL8</i> , <i>PF4</i> , <i>IL10</i> , <i>CCL7</i> , <i>CCL6</i> , <i>IL1B</i> , <i>CSF3R</i> , <i>IL13RA1</i> , <i>IFNGR2</i> , <i>IL1A</i> , <i>CSF1R</i> , <i>TGFBRI</i> , <i>HGF</i> , <i>OSM</i> , <i>CCL12</i> , <i>INHBA</i> , <i>CXCL16</i> , <i>TNFSF12</i> , <i>TNFSF13</i>	<i>CCR9</i> , <i>IL18RI</i> , <i>IL18RAP</i> , <i>XCL1</i>
TLR signaling pathway	16	4.5	1.85E-07	<i>CCL3</i> , <i>TNF</i> , <i>PIK3CB</i> , <i>LY96</i> , <i>TLR1</i> , <i>CXCL9</i> , <i>TLR2</i> , <i>TLR3</i> , <i>TLR4</i> , <i>TLR7</i> , <i>TLR8</i> , <i>FOS</i> , <i>JUN</i> , <i>IL1B</i> , <i>CD14</i> , <i>SPP1</i>	
Chemokine signaling pathway	17	4.8	9.72E-05	<i>CCL3</i> , <i>CCL2</i> , <i>LYN</i> , <i>PIK3CB</i> , <i>HCK</i> , <i>CCR1</i> , <i>CXCL2</i> , <i>CXCL9</i> , <i>CCL9</i> , <i>CCL8</i> , <i>PF4</i> , <i>CCL7</i> , <i>CCL6</i> , <i>CCL12</i> , <i>GNGT2</i> , <i>CXCL16</i> , <i>PAK1</i>	
Ag processing and presentation	8	2.3	0.018	<i>CTSL</i> , <i>LGMN</i> , <i>H2-EB1</i> , <i>IFI30</i> , <i>H2-AB1</i> , <i>CTSB</i> , <i>H2-DMA</i> , <i>CD74</i>	

Genome-wide mRNA expression in IL-10⁺CD8 T cells was analyzed using microarrays and compared with IL-10⁻CD8 T cells. Genes with significant changes were placed into the indicated biological pathways using the KEGG pathway tool in DAVID bioinformatics resources. Genes upregulated or downregulated refers to genes increased or decreased in IL-10⁺CD8 compared with IL-10⁻CD8 T cells.

IL-10 also exhibited a highly activated proinflammatory transcriptional profile.

To validate these results, we analyzed a subset of these differentially regulated genes by qRT-PCR and for protein expression. As shown in Fig. 7A, IL-1 α , IL-1 β , IL-10, CCL2, TLR2, TLR3, TLR4, prosaposin, hexosaminidase A, and perforin mRNA were increased and STAT-4 mRNA was decreased in IL-10⁺CD8 compared with IL-10⁻CD8 T cells, confirming our microarray analysis. As shown in Fig. 4A, some IL-10⁻CD8 T cells were CD69⁺, indicating recent Ag exposure. To confirm that these cells were not hyperactivated, we sorted CD69⁺IL-10⁻, CD69⁺IL-10⁺, and CD69⁻IL-10⁻ CD8 T cells, and compared expression levels of a subset of genes shown in Fig. 7A. CD69⁺IL-10⁺CD8 T cells had increased IL-10, IL-1 α , CCL2, TLR3, and perforin, and decreased STAT-4 mRNA levels compared with CD69⁺IL-10⁻CD8 T cells (Fig. 7B). In addition, we investigated protein expression in IL-10⁺ cells by surface staining for MHC class II and the high-affinity IgE receptor (Fc ϵ R1), and by intracellular staining for LAMP1/2 (CD107a/b) and granzyme B after stimulation with peptide S510. LAMP1/2, granzyme B, MHC class II, and Fc ϵ R1

were all increased in epitope S510-specific IL-10⁺CD8 compared with IL-10⁻CD8 T cells (Fig. 7C), confirming our microarray data. Most importantly, IL-10⁺CD8 T cells were more cytotoxic than IL-10⁻CD8 T cells when examined directly ex vivo for the ability to lyse peptide S510-coated EL4 target cells (Fig. 7D).

IL-10 is protective in J2.2-V-1 demyelinating disease

Demyelination in J2.2-V-1-infected mice is largely immunopathological, with myelin damage occurring during virus clearance (20). The observation that IL-10⁺CD8 T cells were highly activated and cytolytic raised the question whether the IL-10 expressed by these cells would be able to diminish immunopathological changes in the J2.2-V-1-infected CNS.

First, we confirmed a role for IL-10 in J2.2-V-1-infected mice by monitoring survival, weight, and demyelination in age- and sex-matched IL-10^{+/+} and IL-10^{-/-} B6 mice infected with 1500 PFU J2.2-V-1. Infected IL-10^{-/-} mice died at a greater rate than IL-10^{+/+} mice and had increased weight loss (Fig. 8A; days 7–12 p.i.; $p \leq 0.05$). We detected more rapid virus clearance in IL-10^{-/-} mice, showing that the mice had increased ability to control the

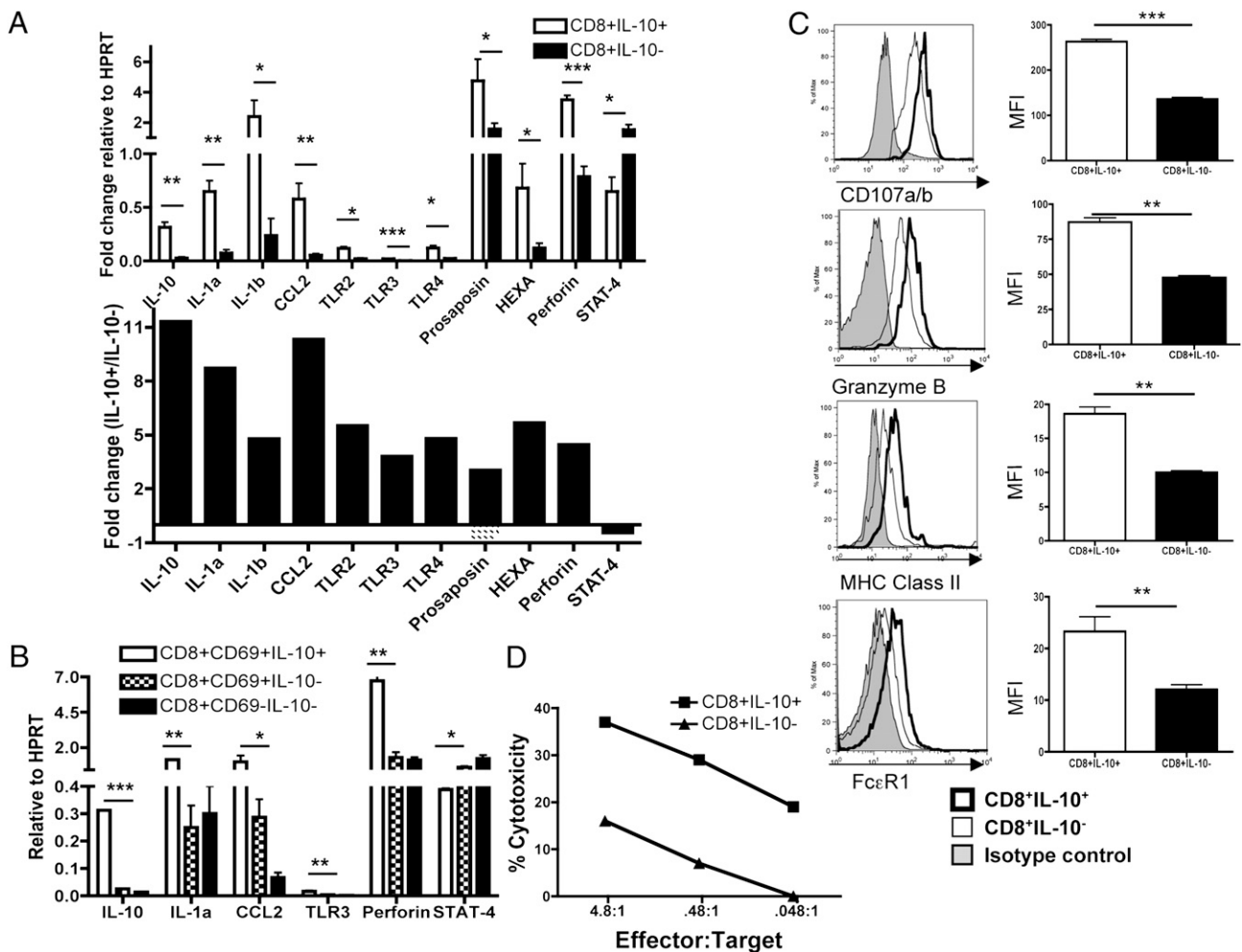


FIGURE 7. qRT-PCR and protein analyses show increased expression of inflammatory pathways in IL-10⁺CD8 T cells compared with IL-10⁻CD8 T cells. *A*, qRT-PCR was performed on IL-10⁺CD8 and IL-10⁻CD8 T cell mRNA purified from CNS-derived lymphocytes. Genes were selected for analysis based on the microarray results. *B*, qRT-PCR was performed on CD69⁺IL-10⁻CD8, CD69⁺IL-10⁺CD8, and CD69⁻IL-10⁻CD8 T cell mRNA purified from CNS-derived lymphocytes. CD69⁺IL-10⁺ and CD69⁺IL-10⁻ CD8 T cell samples were analyzed for statistically significant differences. *C*, CNS-derived lymphocytes from a J2.2-V-1-infected B6 mouse were cultured with S510 peptide for 6 h and then costained with IL-10, CD107a/b (LAMP1/2), and/or granzyme B. Cells from infected Vert-X mice were stained for MHC class II and Fc ϵ R1 expression. All FACS plots are gated on CD8 T cells. *D*, CNS-derived IL-10⁺ and IL-10⁻ CD8 lymphocytes were analyzed for ex vivo cytolytic function using S510-peptide-coated EL4 cells. Effector/target ratios were determined based on percentage of tetramer S510⁺ effector cells. * $p < 0.05$, ** $p < 0.01$, *** $p < 0.001$. Data are representative of two or three separate experiments with a total of 8–12 mice analyzed.

infection. Diminished IL-10 expression is often associated with increased numbers of inflammatory cells present at sites of inflammation (2). Consistent with these results, we found more innate immune effector cells (macrophages, neutrophils, and NK cells) at day 4 p.i. and increased virus-specific CD4 and CD8 T cells at day 8 p.i. (Fig. 9). Thus, increased cellular infiltration in the CNS of IL-10^{-/-} mice enhanced viral clearance, but at the cost of diminishing survival. To assess the role of IL-10 in demyelination, we examined infected spinal cords for myelin destruction at day 21 p.i., the peak of demyelination (37). For these experiments, we infected mice with 500 PFU J2.2-V-1 to enhance survival (Fig. 8B). Demyelination, as assessed by Luxol fast blue staining, was significantly increased in IL-10^{-/-} mice when compared with B6 mice (Fig. 8B).

To directly examine the individual contribution of IL-10 expressed by CD8 T cells, we adoptively transferred virus-immune undepleted or CD8 T cell-enriched splenocytes from IL-10^{+/+} or IL-10^{-/-} mice to IL-10^{-/-} mice 1 d p.i. with 1500 PFU J2.2-V-1. Similar numbers of epitope S510-specific T cells were present in the transferred IL-10^{+/+} and IL-10^{-/-} splenocytes (data not shown). Although there was no difference in survival between mice receiving CD8 T cell-enriched splenocytes from B6 or IL-10^{-/-} mice, there was diminished weight loss and demyelination in mice receiving IL-10-replete compared with IL-

10^{-/-} CD8 T cells (Fig. 8C, 8D; days 9–12 p.i.; $p \leq 0.05$). Thus, IL-10 expressed by CD8 T cells was protective in the context of infection with J2.2-V-1.

Discussion

In this study, we demonstrate that virus-specific CD8 T cells that are most cytotoxic and hyperactivated in mice with acute encephalitis express IL-10 during the height of the inflammatory response. One interpretation of these results is that IL-10 functions in a self-suppressing or localized manner by tempering the immune response induced by these highly activated CD8 T cells. In this scenario, CD8 T cells would self-regulate when viral Ag concentration (Fig. 4B) and inflammatory response reach a certain level, to minimize immunopathological disease (e.g., demyelination) (Fig. 8). Because only the most activated virus-specific cells express IL-10, immunosuppression may not be generalized, but localized to sites where bystander damage would be maximal. IL-10 expression by CD8 T cells was also detected during the peak of inflammation in mice infected with influenza A virus or SV5 (10, 13). Although there is not agreement in all studies (12), inflammation is increased and clinical disease worsens in the absence of IL-10 in both infections. Furthermore, we show that IL-10 expression solely by CD8 T cells was protective in an adoptive transfer system, even though expression was highly

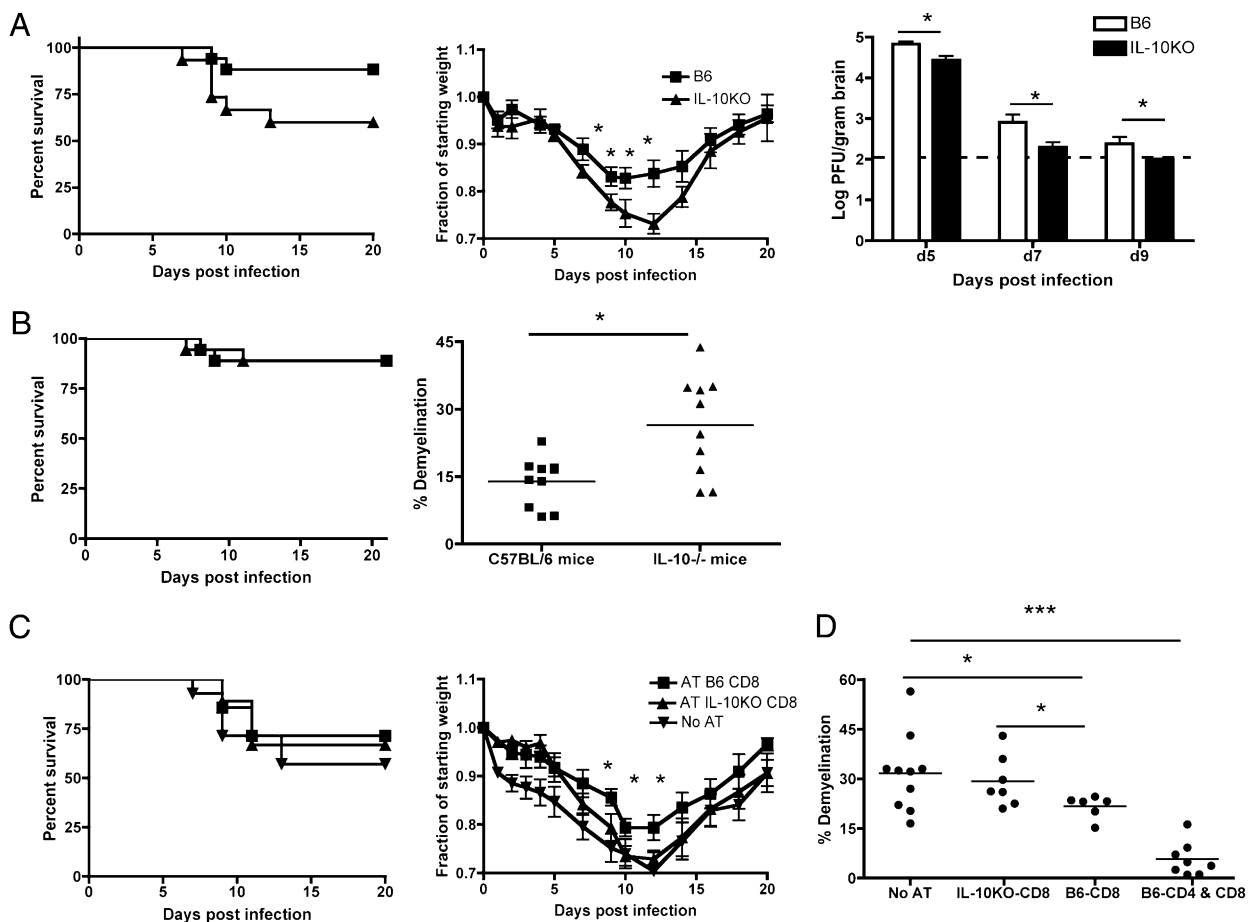


FIGURE 8. IL-10 produced from CD8 T cells is protective in chronic encephalomyelitis. *A*, IL-10^{+/+} and IL-10^{-/-} B6 mice were infected with 1500 PFU J2.2-V-1 and monitored for survival, weight, and virus titers. Dashed line depicts the limit of virus detection. Differences in survival reached statistical significance ($p = 0.02$). *B*, IL-10^{+/+} and IL-10^{-/-} B6 mice were infected with 500 PFU J2.2-V-1 and monitored for survival (left) and spinal cord demyelination at day 21 p.i. Each symbol represents a different mouse. *C* and *D*, IL-10^{-/-} B6 mice were infected with 1500 PFU J2.2-V-1 and received no cells or undepleted or CD8 T cell-enriched splenocytes from virus-immune IL-10^{+/+} or IL-10^{-/-} B6 mice. Mice were monitored for survival and weight loss (*C*), and spinal cord demyelination (*D*). * $p < 0.05$, *** $p < 0.001$. Data are representative of three separate experiments, with a total of 15 mice analyzed.

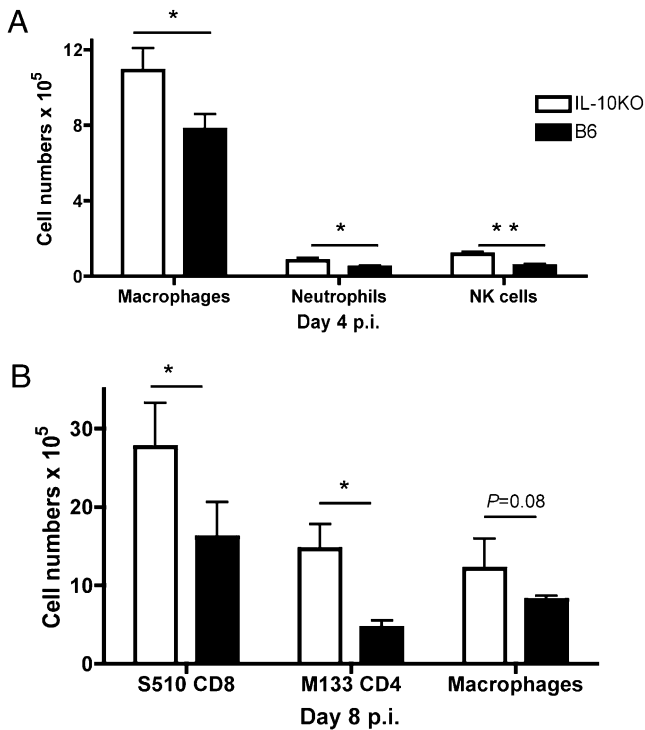


FIGURE 9. IL-10^{-/-} mice have increased brain cell infiltrates compared with IL-10^{+/+} mice. IL-10^{+/+} and IL-10^{-/-} mice were infected with 1500 PFU J2.2-V-1. CNS-derived leukocytes were stained as described in *Materials and Methods* and examined by flow cytometry. Mice were sacrificed at day 4 (A) or 8 p.i. (B). White bars represent IL-10^{-/-} mice; black bars represent IL-10^{+/+} B6 mice. **p* < 0.05, ***p* < 0.01. Data are representative of two separate experiments.

elevated for only a short period (Figs. 1, 8). In addition, expression of IL-10 by these highly activated CD8 cells was dynamic, as shown by the high rate of interconversion of IL-10⁻ and IL-10⁺ populations in vitro and in vivo after adoptive transfer. This plasticity may reflect recent exposure to virus Ag because the IL-10⁺CD8 T cells preferentially expressed CD69 (Fig. 4A). Variable IL-10 expression suggests that exposure to Ag is transitory, possibly reflecting focal distribution of virus Ag in the brain (38). Furthermore, virus is cleared from the brain in a rostral to caudal manner (39, 40), with clearance of inflammatory cells lagging behind that virus (S. Perlman, unpublished observations); cells remaining at sites of virus clearance would have diminished viral Ag exposure resulting in downregulation of IL-10 production. The high activation state of these cells was not a precursor to cell death, because IL-10⁺ cells could be detected for at least 6 d after adoptive transfer.

Until recently, IL-10 has been considered to be most important in chronic infections and autoimmune disease. In animals persistently infected with lymphocytic choriomeningitis virus or *Leishmania* or HCV-infected humans, IL-10 produced by CD4 T cells has been implicated in pathogen persistence (7–9, 41). In these infections, IL-10 was produced by CD4 and not CD8 T cells; this is consistent with our results because IL-10 expression by CD8 T cells rapidly diminishes after day 7 p.i. and is nearly at background levels by 21 d p.i. in the brain, whereas CD4 T cells continue to express IL-10 for at least 42 d p.i. (Fig. 1).

To our knowledge, this is the first report to demonstrate that IL-10 expression in CD8 T cells is dependent on high Ag stimulation and signaling through the ERK1/2 and p38 MAPK pathways (Fig. 4C–E). p38, but not ERK1/2 signaling, was found to be important in IL-10 production in monocytes (42). Conversely,

ERK1/2 signaling but not p38 is required for IL-10 production in all CD4 Th subsets (6, 31). Therefore, IL-10 expression is dependent on MAPK pathways in all tested cells, but exact requirements are cell specific. Although we did not examine the role of JNK of the MAPK pathway in IL-10 expression, its signaling may also be needed for maximal IL-10 production as IL-10⁺ cells showed increased *jun* expression as assessed by gene expression array (Supplemental Table I).

Our results showed that IL-10⁺CD8 T cells were more cytolytic than IL-10⁻CD8 T cells (Fig. 7D). Consistent with these data, genes involved in cytolytic function were increased in IL-10⁺CD8 compared with IL-10⁻CD8 T cells in gene expression analyses (Fig. 7, Table I). Other upregulated genes in IL-10⁺CD8 T cells included several that are involved in the innate immune response and are most commonly expressed by monocytes and macrophages. Some of these proteins, such as the chemokines CCL2, CCL8, CCL12, and CXCL4 (platelet factor 4) and cytokines IL-1 α , IL-1 β , and IL-18 are predicted to enhance the inflammatory response. However, further work will be required to understand why some genes, such as TLRs, C-type lectins, and FcRs, are increased in expression in IL-10⁺CD8 T cells.

Equally interesting is diminished expression of STAT-4 in IL-10⁺CD8 T cells; STAT-4 is required for maximal IL-12–induced IL-10 expression in CD4 T cells (6). CD8 T cell expression of IL-10 is likely to be STAT-4 and thus, IL-12, independent because we found the same frequency of IL-10⁺CD8 T cells in the brains of IL-12R β 2^{-/-} and wild type B6 mice (data not shown). Recently, the transcription factors c-Maf and Ahr (aryl hydrocarbon receptor) were demonstrated to be essential for IL-10 expression by Tr1 CD4 T cells and c-Maf for IL-10 production in macrophages (43, 44). The expression of these transcription factors was not increased in IL-10⁺CD8 T cells, possibly because they may be upregulated only during the early induction phase. Alternatively, different pathways of IL-10 induction may exist in CD4 and CD8 T cells.

In summary, IL-10 is produced by the most highly activated, cytotoxic CD8 T cells in the infected CNS at the peak of inflammation and is protective against morbidity. This study is consistent with the notion that cytotoxic CD8 T cells self-regulate themselves by producing IL-10, and thus that enhanced activation does not invariably result in the development of cells with greater potential for immunopathological disease. Manipulation of IL-10 expression by CD8 T cells might afford another approach to diminishing tissue destruction in animals or humans with acute encephalitis.

Acknowledgments

We thank Drs. John Harty, Hai-Hui Xue, and Jon Houtman for stimulating discussion and critical review of the manuscript. We thank Dr. Tom Bair (University of Iowa DNA facility) for help with gene expression analysis and the National Institutes of Health Tetramer Core Facility (Atlanta, GA) for providing tetramers.

Disclosures

The authors have no financial conflicts of interest.

References

- Sellon, R. K., S. Tonkonogy, M. Schultz, L. A. Dieleman, W. Grentner, E. Balish, D. M. Rennick, and R. B. Sartor. 1998. Resident enteric bacteria are necessary for development of spontaneous colitis and immune system activation in interleukin-10-deficient mice. *Infect. Immun.* 66: 5224–5231.
- Couper, K. N., D. G. Blount, and E. M. Riley. 2008. IL-10: the master regulator of immunity to infection. *J. Immunol.* 180: 5771–5777.
- Moore, K. W., R. de Waal Malefyt, R. L. Coffman, and A. O'Garra. 2001. Interleukin-10 and the interleukin-10 receptor. *Annu. Rev. Immunol.* 19: 683–765.
- Saraiva, M., and A. O'Garra. 2010. The regulation of IL-10 production by immune cells. *Nat. Rev. Immunol.* 10: 170–181.

5. Perona-Wright, G., K. Mohrs, F. M. Szaba, L. W. Kummer, R. Madan, C. L. Karp, L. L. Johnson, S. T. Smiley, and M. Mohrs. 2009. Systemic but not local infections elicit immunosuppressive IL-10 production by natural killer cells. *Cell Host Microbe* 6: 503–512.
6. Saraiva, M., J. R. Christensen, M. Veldhoen, T. L. Murphy, K. M. Murphy, and A. O'Garra. 2009. Interleukin-10 production by Th1 cells requires interleukin-12-induced STAT4 transcription factor and ERK MAP kinase activation by high antigen dose. *Immunity* 31: 209–219.
7. Brooks, D. G., M. J. Trifilo, K. H. Edelmann, L. Teyton, D. B. McGavern, and M. B. Oldstone. 2006. Interleukin-10 determines viral clearance or persistence in vivo. *Nat. Med.* 12: 1301–1309.
8. Ejmaes, M., C. M. Filippi, M. M. Martinic, E. M. Ling, L. M. Togher, S. Crotty, and M. G. von Herrath. 2006. Resolution of a chronic viral infection after interleukin-10 receptor blockade. *J. Exp. Med.* 203: 2461–2472.
9. Belkaid, Y., K. F. Hoffmann, S. Mendez, S. Kamhawi, M. C. Udey, T. A. Wynn, and D. L. Sacks. 2001. The role of interleukin (IL)-10 in the persistence of *Leishmania major* in the skin after healing and the therapeutic potential of anti-IL-10 receptor antibody for sterile cure. *J. Exp. Med.* 194: 1497–1506.
10. Palmer, E. M., B. C. Holbrook, S. Arimilli, G. D. Parks, and M. A. Alexander-Miller. 2010. IFN γ -producing, virus-specific CD8⁺ effector cells acquire the ability to produce IL-10 as a result of entry into the infected lung environment. *Virology* 404: 225–230.
11. Spender, L. C., T. Hussell, and P. J. Openshaw. 1998. Abundant IFN- γ production by local T cells in respiratory syncytial virus-induced eosinophilic lung disease. *J. Gen. Virol.* 79: 1751–1758.
12. McKinsty, K. K., T. M. Strutt, A. Buck, J. D. Curtis, J. P. Dibble, G. Huston, M. Tighe, H. Hamada, S. Sell, R. W. Dutton, and S. L. Swain. 2009. IL-10 deficiency unleashes an influenza-specific Th17 response and enhances survival against high-dose challenge. *J. Immunol.* 182: 7353–7363.
13. Sun, J., R. Madan, C. L. Karp, and T. J. Braciale. 2009. Effector T cells control lung inflammation during acute influenza virus infection by producing IL-10. *Nat. Med.* 15: 277–284.
14. Bergmann, C. C., T. E. Lane, and S. A. Stohlman. 2006. Coronavirus infection of the central nervous system: host-virus stand-off. *Nat. Rev. Microbiol.* 4: 121–132.
15. Stohlman, S. A., C. C. Bergmann, and S. Perlman. 1998. Mouse hepatitis virus. In *Persistent viral infections*. R. Ahmed, and I. Chen, eds. John Wiley & Sons, Ltd., New York. p. 537–557.
16. Zhao, J., J. Zhao, and S. Perlman. 2009. De novo recruitment of antigen-experienced and naive T cells contributes to the long-term maintenance of antiviral T cell populations in the persistently infected central nervous system. *J. Immunol.* 183: 5163–5170.
17. Madan, R., F. Demircik, S. Surianarayanan, J. L. Allen, S. Divanovic, A. Trompette, N. Yogev, Y. Gu, M. Khodoun, D. Hildeman, et al. 2009. Non-redundant roles for B cell-derived IL-10 in immune counter-regulation. *J. Immunol.* 183: 2312–2320.
18. Trandem, K., D. Anghelina, J. Zhao, and S. Perlman. 2010. Regulatory T cells inhibit T cell proliferation and decrease demyelination in mice chronically infected with a coronavirus. *J. Immunol.* 184: 4391–4400.
19. Xue, S., N. Sun, N. Van Rooijen, and S. Perlman. 1999. Depletion of blood-borne macrophages does not reduce demyelination in mice infected with a neurotropic coronavirus. *J. Virol.* 73: 6327–6334.
20. Wu, G. F., A. A. Dandekar, L. Pewe, and S. Perlman. 2000. CD4 and CD8 T cells have redundant but not identical roles in virus-induced demyelination. *J. Immunol.* 165: 2278–2286.
21. Kapil, P., R. Atkinson, C. Ramakrishna, D. J. Cua, C. C. Bergmann, and S. A. Stohlman. 2009. Interleukin-12 (IL-12), but not IL-23, deficiency ameliorates viral encephalitis without affecting viral control. *J. Virol.* 83: 5978–5986.
22. Lin, M. T., D. R. Hinton, B. Parra, S. A. Stohlman, and R. C. van der Veen. 1998. The role of IL-10 in mouse hepatitis virus-induced demyelinating encephalomyelitis. *Virology* 245: 270–280.
23. Templeton, S. P., and S. Perlman. 2007. Pathogenesis of acute and chronic central nervous system infection with variants of mouse hepatitis virus, strain JHM. *Immunol. Res.* 39: 160–172.
24. Williamson, J. S., K. C. Sykes, and S. A. Stohlman. 1991. Characterization of brain-infiltrating mononuclear cells during infection with mouse hepatitis virus strain JHM. *J. Neuroimmunol.* 32: 199–207.
25. Haring, J. S., L. L. Pewe, and S. Perlman. 2001. High-magnitude, virus-specific CD4 T-cell response in the central nervous system of coronavirus-infected mice. *J. Virol.* 75: 3043–3047.
26. O'Garra, A., and K. M. Murphy. 2009. From IL-10 to IL-12: how pathogens and their products stimulate APCs to induce T(H)1 development. *Nat. Immunol.* 10: 929–932.
27. Landais, E., P. A. Romagnoli, A. L. Corper, J. Shires, J. D. Altman, I. A. Wilson, K. C. Garcia, and L. Teyton. 2009. New design of MHC class II tetramers to accommodate fundamental principles of antigen presentation. *J. Immunol.* 183: 7949–7957.
28. Held, K. S., W. G. Glass, Y. I. Orlovsky, K. A. Shamberger, T. D. Petley, P. J. Branigan, J. M. Carton, H. S. Beck, M. R. Cunningham, J. M. Benson, and T. E. Lane. 2008. Generation of a protective T-cell response following coronavirus infection of the central nervous system is not dependent on IL-12/23 signaling. *Viral Immunol.* 21: 173–188.
29. Anghelina, D., L. Pewe, and S. Perlman. 2006. Pathogenic role for virus-specific CD4 T cells in mice with coronavirus-induced acute encephalitis. *Am. J. Pathol.* 169: 209–222.
30. Kaech, S. M., and E. J. Wherry. 2007. Heterogeneity and cell-fate decisions in effector and memory CD8⁺ T cell differentiation during viral infection. *Immunity* 27: 393–405.
31. Dong, C., R. J. Davis, and R. A. Flavell. 2002. MAP kinases in the immune response. *Annu. Rev. Immunol.* 20: 55–72.
32. Klein, P. J., C. M. Schmidt, C. A. Wiesenauer, J. N. Choi, E. A. Gage, M. T. Yip-Schneider, E. A. Wiebke, Y. Wang, C. Omer, and J. S. Sebolt-Leopold. 2006. The effects of a novel MEK inhibitor PD184161 on MEK-ERK signaling and growth in human liver cancer. *Neoplasia* 8: 1–8.
33. Gallagher, T. F., G. L. Seibel, S. Kassus, J. T. Laydon, M. J. Blumenthal, J. C. Lee, D. Lee, J. C. Boehm, S. M. Fier-Thompson, J. W. Abt, et al. 1997. Regulation of stress-induced cytokine production by pyridinylimidazoles; inhibition of CSBP kinase. *Bioorg. Med. Chem.* 5: 49–64.
34. Davies, S. P., H. Reddy, M. Caivano, and P. Cohen. 2000. Specificity and mechanism of action of some commonly used protein kinase inhibitors. *Biochem. J.* 351: 95–105.
35. Groux, H., M. Bigler, J. E. de Vries, and M. G. Roncarolo. 1998. Inhibitory and stimulatory effects of IL-10 on human CD8⁺ T cells. *J. Immunol.* 160: 3188–3193.
36. Santin, A. D., P. L. Hermonat, A. Ravaggi, S. Bellone, S. Pecorelli, J. J. Roman, G. P. Parham, and M. J. Cannon. 2000. Interleukin-10 increases Th1 cytokine production and cytotoxic potential in human papillomavirus-specific CD8⁽⁺⁾ cytotoxic T lymphocytes. *J. Virol.* 74: 4729–4737.
37. Wang, F. L., D. R. Hinton, W. Gilmore, M. D. Trousdale, and J. O. Fleming. 1992. Sequential infection of glial cells by the murine hepatitis virus JHM strain (MHV-4) leads to a characteristic distribution of demyelination. *Lab. Invest.* 66: 744–754.
38. Barnett, E. M., M. D. Cassell, and S. Perlman. 1993. Two neurotropic viruses, herpes simplex virus type 1 and mouse hepatitis virus, spread along different neural pathways from the main olfactory bulb. *Neuroscience* 57: 1007–1025.
39. Perlman, S., G. Jacobsen, and A. Afifi. 1989. Spread of a neurotropic murine coronavirus into the CNS via the trigeminal and olfactory nerves. *Virology* 170: 556–560.
40. Perlman, S., G. Evans, and A. Afifi. 1990. Effect of olfactory bulb ablation on spread of a neurotropic coronavirus into the mouse brain. *J. Exp. Med.* 172: 1127–1132.
41. Brady, M. T., A. J. MacDonald, A. G. Rowan, and K. H. Mills. 2003. Hepatitis C virus non-structural protein 4 suppresses Th1 responses by stimulating IL-10 production from monocytes. *Eur. J. Immunol.* 33: 3448–3457.
42. Foey, A. D., S. L. Parry, L. M. Williams, M. Feldmann, B. M. Foxwell, and F. M. Brennan. 1998. Regulation of monocyte IL-10 synthesis by endogenous IL-1 and TNF- α : role of the p38 and p42/44 mitogen-activated protein kinases. *J. Immunol.* 160: 920–928.
43. Apetoh, L., F. J. Quintana, C. Pot, N. Joller, S. Xiao, D. Kumar, E. J. Burns, D. H. Sherr, H. L. Weiner, and V. K. Kuchroo. 2010. The aryl hydrocarbon receptor interacts with c-Maf to promote the differentiation of type 1 regulatory T cells induced by IL-27. *Nat. Immunol.* 11: 854–861.
44. Cao, S., J. Liu, L. Song, and X. Ma. 2005. The protooncogene c-Maf is an essential transcription factor for IL-10 gene expression in macrophages. *J. Immunol.* 174: 3484–3492.